Nanoscale Res Lett (2008) 3:338–342
DOI 10.1007/s11671-008-9162-0

NANO PERSPECTIVES

Preparation and Characteraction of New Magnetic Co–Al HTLc/Fe_3O_4 Solid Base

Jun Wang · Jia You · Zhanshuang Li · Piaoping Yang · Xiaoyan Jing · Milin Zhang

Received: 9 May 2008 / Accepted: 18 August 2008 / Published online: 5 September 2008

Abstract Novel magnetic hydrotalcite-like compounds (HTLcs) were synthesized through introducing magnetic substrates (Fe_3O_4) into the Co–Al HTLcs materials by hydrothermal method. The magnetic Co–Al HTLcs with different Fe_3O_4 contents were characterized in detail by XRD, FT-IR, SEM, TEM, DSC, and VSM techniques. It has been found that the magnetic substrates were incorporated with HTLcs successfully, although the addition of Fe_3O_4 might hinder the growth rate of the crystal nucleus. The morphology of the samples showed the relatively uniform hexagonal platelet-like sheets. The grain boundaries were well defined with narrow size distribution. Moreover, the Co–Al HTLcs doped with magnetic substrates presented the paramagnetic property.

Keywords Magnetic Co–Al hydrotalcite · Hydrothermal method · Paramagnetism · Nanoparticles · X-ray techniques

Introduction

Hydrotalcite-like compounds (HTLcs) are a family of two-dimensional nanostructured lamellar ionic compounds, which contains positively charged layers and exchangeable anion in the interlayer [1–3]. Recently, HTLcs have received considerable attention in view of their potential usefulness as catalysts and catalyst precursors, as well as for applications in areas as diverse as medicine science, ion exchangers, oil field exploration, or sorption processes [4–7]. However, the separation and recovery of these solid base mixed oxides from the reaction products are still difficult. So a large amount of separation energy and cost are consumed for the extra equipment and treatments for separation and recovery. Therefore, it is essential to synthesize a novel solid base catalyst to extend the utility of catalysts and develop green routes. To date, most attention is put on investigating the magnetic properties of brucite-type hydroxides of general formula $M^{2+}n(OH)m(A)p$ (A is generally a carboxylate or dicarboxylate anion), as these layered materials present ferro-, ferri-, antiferro-, or unusual metamagnetic behaviors. For example, Pérez-Ramírez et al [8] reported the magnetic behavior of Co–Al, Ni–Al, and Mg–Al hydrotalcites, as well as the mixed oxides obtained after calcination. Trujillano et al. [9] reported the magnetic properties of a series of layered Cu–Al hydroxides intercalated with alkylsulfonates. Carja et al. [10] reported new magnetic layered structures which can be used as precursors for new hybrid nanostructures, such as aspirin-hydrotalcite-like anionic clays.

In the present work, we designed and synthesized magnetic Co–Al HTLcs through introducing magnetic Fe_3O_4 nanoparticles using the hydrothermal method in autoclaves under autogenous water vapor pressure at 180 °C for 6 h. However, up to our best knowledge, such a study has not been carried out on hydrotalcite. The magnetic HTLcs materials with super-paramagnetism make them possible to achieve the ease of recovery, waste generation, environmental friendliness, and recycling of HTLcs through the external rotating magnetic field. This

J. Wang (✉) · Z. Li · P. Yang · X. Jing · M. Zhang
College of Material Science and Chemical Engineering, Harbin Engineering University, Harbin 150001, P. R. China
e-mail: zhqw1888@sohu.com

J. Wang · Z. Li · P. Yang · X. Jing · M. Zhang
The Key Laboratory of Superlight Materials and Surface Technology, Ministry of Education, Harbin 150001, P. R. China

J. You
The 49th Research Institute of China Electronics Technology Group, Harbin 150001, P. R. China

novel magnetic HTLcs are expected to act as green catalyst and hence solve the above mentioned disadvantages.

Experimental Section

Synthesis

Magnetic nanoparticles were prepared by dissolving 0.01 mol of $FeSO_4$ and 0.01 mol of $Fe_2(SO_4)_3$ in water solution under stirring at 45 °C, and 20 wt% of $NH_3 \cdot H_2O$ were added dropwise together at a constant pH value of 10–11. The obtained material (Fe_3O_4) was recovered, washed several times with deionized water until the pH was neutral. The obtained Fe_3O_4 was preserved as suspension.

Magnetic Co–Al HTLcs was prepared by the hydrothermal process. An aqueous solution containing 0.40 M $Co(NO_3)_2 \cdot 6H_2O$ and 0.13 M $Al(NO_3)_3 \cdot 9H_2O$ was added dropwise to Fe_3O_4 solution with Fe/Co molar ratio equal to 0.01, 0.02, 0.05, and 0.2, respectively, under vigorous stirring. During the synthesis, the temperature was maintained at 60 °C and pH at about 11 by the simultaneous addition of NaOH and Na_2CO_3 solution. Then the mixture was transferred to an autoclave pressure vessel and hydrothermally treated at 180 °C for 6 h. The autoclave was then cooled down to room temperature. The resulting solid products were separated by filtration, washed with distilled water, and dried at 80 °C for 24 h.

Characteraction

Powder X-ray diffraction (XRD) data were collected in the 2θ range of 5–75° on a Rigaku D/max-IIIB diffractometer using Cu Kα radiation ($\lambda = 1.5406$ Å). FT-IR spectrum was recorded on a Nicolet 5DX spectrophotometer using KBr pellet technique. Transmission electron microscopy (TEM) experiment was performed on a PHILIPS CM 200 FEG electron microscope with an acceleration voltage of 200 kV. The samples were dispersed in ethanol, and carbon-coated copper grids were used as the sample holder. Scanning electron microscopy (SEM) was performed on a Japan JEOL JSM-6480A instrument at an acceleration voltage of 20 kV and a working distance of 10 mm. Thermogravimetry-differential scanning calorimetry (DSC) was performed on a NEZSCH STA 409PC thermoanalyzer in the temperature range of 40–600 °C with a heating rate of 10 °C/min. Magnetic hysteresis loops were measured using a vibrating sample magnetometer (VSM, JDAW-2000). The nickel, aluminum, and iron contents were determined by inductively coupled plasma mass spectrometry (ICP-MS) emission spectroscopy.

Results and Discussion

XRD

The XRD patterns of magnetic Co–Al HTLcs with different Fe/Co ratios were shown in Fig. 1. All the XRD patterns of the samples showed the typical reflections of the basal (003), (006), (009), (015), (110), and (113) planes [11]. As seen in the Fig. 1, these diffraction peaks became less narrow and intense with the increase of Fe/Co ratios. The results indicated that the addition of Fe_3O_4 might hinder the growth rate of the crystal nucleus. For the Fe_3O_4-containing samples, the third peak corresponding to the basal (009) plane was divided into two distinct peaks. The first one, recorded at lower diffraction angles corresponds to the basal spacing (009), whereas the second one might come from the Fe_3O_4. Moreover, the unchangeable intersheet spacing (d_{003}) presented that the magnetism (Fe_3O_4) was highly dispersed in the hydrotalcite structure. Assuming a 3R polytypism for the hydrotalcite, the lattice parameters a and c have been calculated from the positions of the XRD peaks [12]. The lattice parameters of the samples were presented in Table 1. The c and a values were quite similar for all the samples, and the differences found can be within experimental error. The element chemical analysis data for magnetic Co–Al HTLcs with different Fe/Co ratios were given in Table 2. As seen in Table 2, the values of the Co/Al ratio for magnetic hydrotalcite with lower Fe/Co ratio were close to the expected one. The result was consistent with the XRD analysis.

TEM and SEM

The morphology of magnetic Co–Al HTLcs was investigated by SEM and TEM and the images were shown in

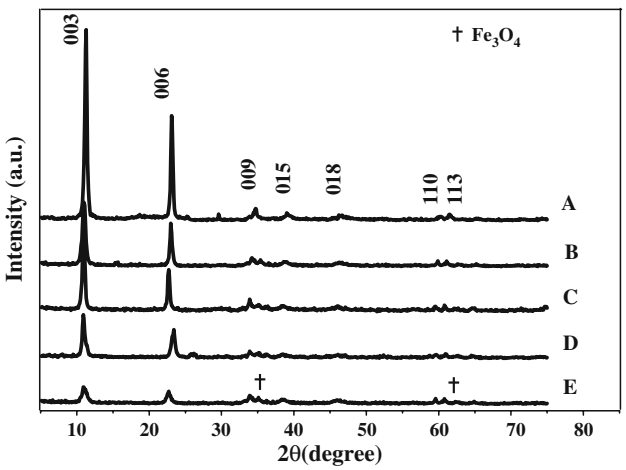

Fig. 1 Powder XRD patterns of magnetic Co–Al HTLcs with different Fe/Co ratios. (a) 0, (b) 0.01, (c) 0.02, (d) 0.05, (e) 0.2

Table 1 Crystal structure parameters of magnetic Co–Al HTLcs with different Fe/Co ratios

Fe/Co ratio	$d_{[003]}$ (nm)	$c_{[003]}$ (nm)	$d_{[006]}$ (nm)	$c_{[006]}$ (nm)	$d_{[110]}$ (nm)	a (nm)
0	0.7695	2.3005	0.3873	1.1619	0.1538	0.3076
0.01	0.7937	2.3811	0.3853	1.1559	0.1538	0.3076
0.02	0.8021	2.4063	0.3873	1.1619	0.1554	0.3108
0.05	0.8195	2.4585	0.3815	1.1445	0.1546	0.3092
0.2	0.7882	2.3646	0.3925	1.1775	0.1546	0.3092

Table 2 Elemental analysis results for the synthesized compounds

Fe/Co ratios	x_m [a]	x [b]	Co (%)[c]	Al (%)[c]	Fe (%)[c]
0.20	3.0	3.5	17.08	2.25	1.95
0.05	3.0	3.1	20.35	3.04	1.02
0.02	3.0	3.1	21.13	3.12	0.48
0.01	3.0	3.2	22.58	3.25	0.23

[a] x_m is the molar ratio of bivalent cations to trivalent cations in initial solutions; [b] x is the molar ratio of bivalent cations to trivalent cations in as-prepared solid samples; [c]Elemental analysis by ICP-MS in weight percentage

Fig. 2. As shown in Fig. 2, all the Fe_3O_4-containing particles consisted of relatively uniform hexagonal platelet-like sheets. The grain boundaries were well-defined with narrow size distribution. No diffraction fringes were observed, although the sample was crystalline, as evidenced by the XRD pattern.

FT-IR

Figure 3 displayed FT-IR spectra of the magnetic hydrotalcites samples with different Fe/Co ratios. A broad absorption band centered at $\approx$3,470 cm^{-1} present in all samples is attributed to O–H stretching vibration of hydrogen-bonded hydroxyl groups in the brucite-like sheets and of water in the interlayer space [13, 14]. Water-bending vibrations of the interlayer water were observed for all samples at 1,632 cm^{-1}. It was noted that the strong absorption bands at 1,470 cm^{-1} can be indexed to the v_3 mode of CO_3^{2-} ions. The intensity of this band became weaker when the Fe_3O_4 intercalate into the HTlcs. The other bands at 1,040 and 864 cm^{-1}were characterized to the v_1 and v_2 modes of the carbonate ion, respectively. Besides, an absorption band at 662 cm^{-1} in Fig. 2a was ascribed to Co–O stretching. Such a band was also present in the spectra for the magnetic hydrotalcites samples, but centered in a lower wavenumber region, 617 cm^{-1}. Finally, the bands at wavenumbers 417 cm^{-1} were attributed to Fe–OH vibrations.

DSC

To examine the thermal stability of as-synthesized sample during calcination, the Thermogravimetry-differential scanning calorimetry analysis was carried out in nitrogen. The DSC curves of hydrotalcites samples with different Fe/Co ratios were shown in Fig. 4. As seen in Fig. 4, all the DSC profiles exhibited two apparent endothermic events which were in agreement with the typical decomposition mechanism of HTLcs [15]. The first endothermal peak at lower temperature can be assigned to the desorption of the loss of interlayer water. The second endothermal peak at higher temperatures ($T > 250$ °C) was related to the decomposition (dehydroxylation) of the hydroxide layers and the removal of anions (carbonate) in the brucite-like

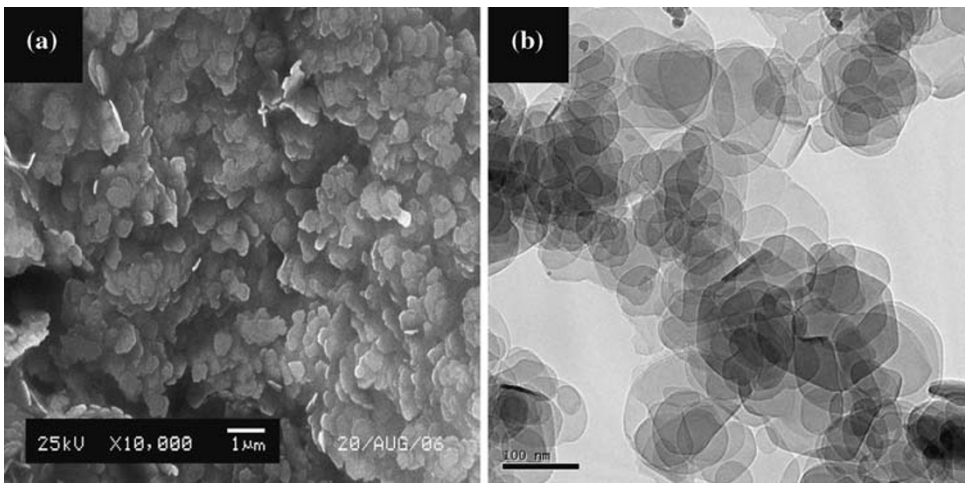

Fig. 2 SEM (**a**) and TEM (**b**) images of magnetic Co–Al HTLcs

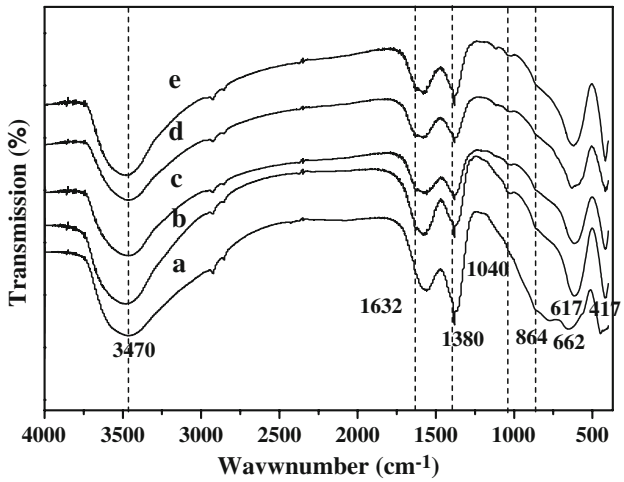

Fig. 3 FT-IR spectra of magnetic Co–Al HTLcs with different Fe/Co ratios. (a) 0, (b) 0.01, (c) 0.02, (d) 0.05, (e) 0.2

layers [16, 17]. It was interesting to note that, when the Fe/Co ratio was higher than 0.05, the two endothermic bands were shifted toward higher combustion temperatures. This observation can be related to the pillared effect of Fe_3O_4 in the layer of HTlcs.

VSM

The magnetic hysteresis curve of magnetic Co–Al HTLcs (Fe/Co = 0.2) performed at room temperature was depicted in Fig. 5. The magnetic capabilities of Co–Al HTLcs with different Fe/Co ratios were given in Table 3. As displayed in the figure, the magnetic curves increased linearly with increasing field at low magnetization, while the magnetic curves increased slightly with further increasing field, and finally maintained in the fixed value. The hysteresis loop of all the samples exhibited typical characteristic of paramagnetic materials with coercivity

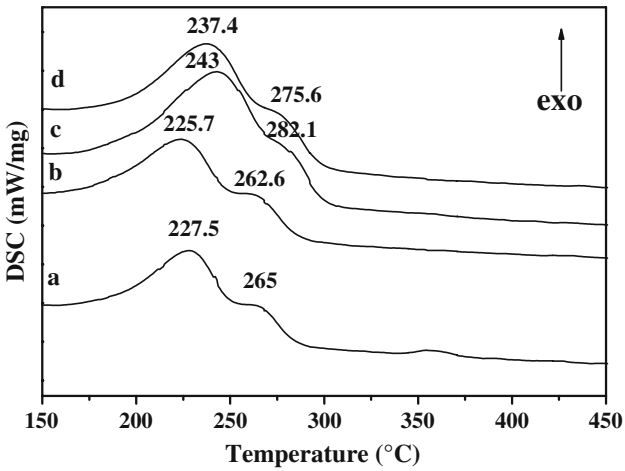

Fig. 4 DSC curves of magnetic Co–Al HTLcs with different Fe/Co ratios. (a) 0.01, (b) 0.02, (c) 0.05, (d) 0.2

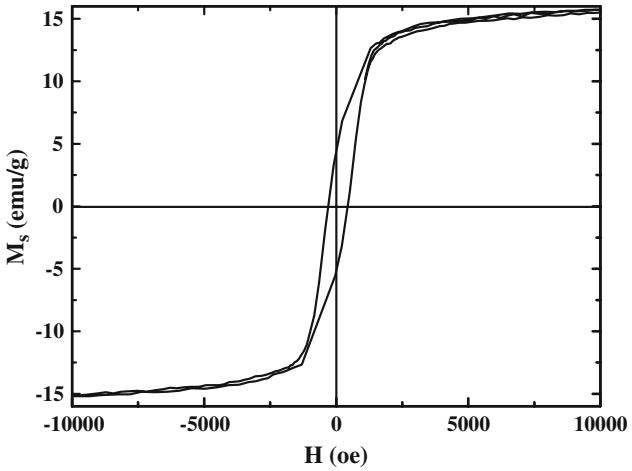

Fig. 5 Magnetic hysteresis curve of magnetic Co–Al HTLcs (Fe/Co = 0.2) measured at room temperature

Table 3 Magnetic property of magnetic Co–Al HTLcs with different Fe/Co ratios

Fe/Co ratios	Saturation magnetization (emu/g)	Coercivity (Oe)
0.20	15.60	0
0.05	7.79	0
0.02	4.63	0
0.01	0.98	0

(Hc) values of 0 Oe. The emerging of paramagnetism at room temperature may be due to the Fe_3O_4 particle with very small particle size [18]. As seen in Table 3, the value of saturation magnetization decreased from 15.6 to 0.98 emu/g with the decrease of Fe/Co ratios because of the change of particle size of the magnetic Co–Al HTLcs.

Conclusions

In summary, magnetic Co–Al HTLcs has been successfully synthesized through hydrothermal method. On the basis of XRD investigations, it has been found that the magnetic substrate (Fe_3O_4) was introduced into the structure of HTLcs. This result was also detected in FT-IR analysis. DSC method revealed that when the Fe/Co ratio was higher than 0.05, the exothermic bands were shifted toward higher combustion temperatures. Moreover, the introduction of Fe_3O_4 endowed the composites with paramagnetism. We expected such novel material has promising applications as the green catalysts or catalyst supporters.

Acknowledgment Financial support from the Key Technology R&D program of Heilongjiang Province (no. G202A423) and Science Fund for Young Scholar of Harbin City (no. 2004AFQXJ038) are greatly acknowledged.

References

1. Z.P. Xu, H.C. Zeng, Chem. Mater. **11**, 67 (1999). doi:10.1021/cm980420b
2. R. Xu, H.C. Zeng, Chem. Mater. **13**, 297 (2001). doi:10.1021/cm000526i
3. M.R. Pérez, I. Pavlovic, C. Barriga, J. Cornejo, M.C. Hermosín, M.A. Ulibarri, Appl. Clay Sci. **32**, 245 (2006). doi:10.1016/j.clay.2006.01.008
4. B.M. Choudary, M. Lakshmi Kantam, A. Rahman, Ch. Venkat Reddy, K. Koteswara Rao, Angew. Chem. Int. Ed. **40**, 763 (2001). doi:10.1002/1521-3773(20010216)40:4<763::AID-ANIE7630>3.0.CO;2-T
5. B.M. Choudary, M. Lakshmi Kantam, A. Rahman, Ch. Venkat Reddy, J. Mol. Catal. Chem. **206**, 145 (2003). doi:10.1016/S1381-1169(03)00413-8
6. J.N. Armor, T.A. Braymer, T.S. Farris, Y. Li, F.P. Petrocelli, E.L. Weist, S. Kannan, C.S. Swamy, Appl. Catal. B Environ. **7**, 397 (1996). doi:10.1016/0926-3373(95)00048-8
7. F. Cavani, F. Trifiró, A. Vaccari, Catal. Today **11**, 173 (1991). doi:10.1016/0920-5861(91)80068-K
8. J. Pérez-Ramírez, A. Ribera, F. Kapteijn, E. Coronado, C.J. Gómez-García, J. Mater. Chem. **12**, 2370 (2002). doi:10.1039/b110314h
9. R. Trujillano, M.J. Holgado, F. Pigazo, V. Rives, Phys. B **373**, 267 (2006). doi:10.1016/j.physb.2005.11.154
10. G. Carja, H. Chiriac, N. Lupu, J. Magn. Magn. Mater. **311**, 26 (2007). doi:10.1016/j.jmmm.2006.11.161
11. Z.P. Xu, R. Xu, H.C. Zeng, Nano. Lett. **1**, 703 (2001). doi:10.1021/nl010045d
12. J. Pérez-Ramírez, G. Mul, F. Kapteijn, J.A. Moulijn, J. Mater. Chem. **11**, 821 (2001). doi:10.1039/b009320n
13. J.M. Fernandez, C. Barriga, M.A. Ulibarri, F.M. Labajos, V. Rives, J. Mater. Chem. **4**, 1117 (1994). doi:10.1039/jm9940401117
14. L. Ji, J. Lin, H.C. Zeng, J. Phys. Chem. B. **104**, 1783 (2000). doi:10.1021/jp993400l
15. J. Pérez-Ramírez, G. Mul, J.A. Moulijn, Vib. Spectrosc. **27**, 75 (2001). doi:10.1016/S0924-2031(01)00119-9
16. S.K. Yun, T.J. Pinnavaia, Inorg. Chem. **35**, 6853 (1996). doi:10.1021/ic960287u
17. K. Takehira, T. Kawabata, S. Shishido, K. Murakami, T. Ohi, D. Shoro, M. Honda, K. Takaki, J. Catal. **231**, 92 (2005). doi:10.1016/j.jcat.2005.01.025
18. J. Gass, P. Poddar, J. Almand, S. Srinath, H. Srikanth, Adv. Funct. Mater. **16**, 71 (2006). doi:10.1002/adfm.200500335